INSTITUTE OF PHYSICS PUBLISHING PHYSICS IN MEDICINE AND BIOLOGY

Phys. Med. Biol. **51** (2006) 1693–1706 doi:10.1088/0031-9155/51/7/004

Fast Monte Carlo simulation of DNA damage formed by electrons and light ions

V A Semenenko and R D Stewart

School of Health Sciences, Purdue University, West Lafayette, IN 47907-2051, USA

E-mail: trebor@purdue.edu

Received 1 November 2005, in final form 31 January 2006
Published 7 March 2006
Online at stacks.iop.org/PMB/51/1693

Abstract

The passage of ionizing radiation through living organisms initiates physical and chemical processes that create clusters of damaged nucleotides within one or two turns of the DNA. These clusters are widely considered an important initiating event for the induction of other biological endpoints, including cell killing and neoplastic transformation. Monte Carlo simulations of the DNA damage formation process are a useful adjunct to experiments because they provide additional information about the spatial configuration of damage within a cluster. In this paper, the fast Monte Carlo damage simulation (MCDS) algorithm is re-parameterized so that yields of double-strand breaks, single-strand breaks and sites of multiple base damage can be simulated for electrons, protons and α particles with kinetic energies on the order of GeV. The MCDS algorithm provides a useful, quasi-phenomenological scheme to interpolate damage yields from computationally expensive, but more detailed, track-structure simulations. The predicted characteristics of various classes of damage produced by electrons, protons and α particles, such as average number of lesions per DNA damage cluster and cluster length in base pairs, are presented. A study examining the effects on damage complexity of an extrinsic free radical scavenger, dimethyl sulfoxide, is also presented. The reported studies provide new information that will aid efforts to characterize the relative biological effectiveness of high-energy protons and other light ions, which are sometimes used in particle therapy for the treatment of cancer.

1. Introduction

The amount and spatial configuration of damage formed in nuclear DNA by the passage of ionizing radiation is widely regarded as an important initiating event for radiobiological endpoints, such as cell killing and neoplastic transformation. Although experimental methods can be used to quantify the overall yields of double-strand breaks (DSBs), single-strand breaks

(SSBs) and some types of base damage (Ward 1998), measurements do not provide information about the exact location of the lesions within the DNA. Computational approaches based on track-structure calculations superimposed on high-order models of DNA (Tomita *et al* 1994, Holley and Chatterjee 1996, Nikjoo *et al* 1994, 1997, 1999, 2001, 2002, Friedland *et al* 2003, 2005) are capable of providing information about damage to individual nucleotides, but ultimately rely on adjustable parameters to relate the spatial distribution of energy deposits to damage formation. Estimates of the adjustable parameters used in track-structure calculations are determined from measured yields of selected types of DNA damage, usually SSBs and DSBs.

Because detailed information about the nature of the damage formed by ionizing radiation is needed for DNA repair studies (Semenenko *et al* 2005, Semenenko and Stewart 2005) and because track-structure simulations are computationally expensive, we developed a fast, quasi-phenomenological Monte Carlo damage simulation (MCDS) algorithm capable of predicting the full spectrum of damage produced by electrons, protons and α particles (Semenenko and Stewart 2004). We refer to the MCDS algorithm as a quasi-phenomenological model because an *ad hoc* procedure is used to determine the spatial clustering of lesions within the DNA even though the induction of base damage and strand breaks is explicitly simulated. The main advantage of the *ad hoc* lesion clustering procedure is that the computational expense of simulating the initial physical and chemical processes that result in DNA damage is avoided, i.e., the MCDS algorithm is very fast compared to track-structure simulations. Depending on particle type and energy, the simulation of DNA damage configurations in 1000 cells using the MCDS algorithm only takes between 4.3 and 15.6 s (lower energies take less CPU time) on a 2.8 GHz Intel ® Pentium III Xeon computer.

In Semenenko and Stewart (2004), the four adjustable parameters used in the MCDS algorithm were estimated using damage yields from track-structure simulations for 4.5 keV electrons, 0.3–4 MeV protons and 2–10 MeV α particles (Nikjoo *et al* 1999, 2001). Because of the phenomenological nature of the MCDS algorithm, the predicted damage yields were of questionable validity for higher energy ions, which are of interest for applications such as proton therapy for the treatment of cancer. In proton therapy, initial kinetic energies may range from 60 to 250 MeV depending on the type and location of the tumour (Amaldi and Kraft 2005). In this paper, we demonstrate that the MCDS algorithm can be re-parameterized in a way that provides a unified framework to interpolate and extend DNA damage yields predicted by detailed track-structure simulations for light ions and electrons. The reported studies also suggest that the re-parameterized version of the MCDS algorithm can provide plausible estimates of damage configurations for particle energies into the GeV range.

2. Methods

2.1. Fast Monte Carlo damage simulation algorithm

The MCDS algorithm is described in detail elsewhere (Semenenko and Stewart 2004). Briefly, simulations are performed in two major steps: (1) randomly distribute in a DNA segment the expected number of lesions[1] produced in a cell per Gy of radiation and (2) subdivide the lesions in the segment into clusters. DNA segment length is given by a parameter n_{seg} expressed in units of base pairs (bp) Gy^{-1} cell^{-1}. This segment length is an *ad hoc* parameter and should not be considered equivalent to the DNA content of a specific chromosome or cell. The number of lesions to be distributed within the segment is given by the sum of the number of

[1] Note the change of terminology in comparison with Semenenko and Stewart (2004): elementary damages are now referred to as lesions, and lesions are referred to as clusters.

strand breaks Gy^{-1} $cell^{-1}$, σ_{Sb} and the number of base damages Gy^{-1} $cell^{-1}$, $\sigma_{Bb} = f\sigma_{Sb}$, where f is the base damage to strand break ratio. Finally, the grouping of lesions into clusters is determined by a parameter N_{min} (bp), which specifies the minimum length of undamaged DNA between neighbouring lesions such that these lesions are said to belong to two different clusters (some 'clusters' may contain only one lesion). The MCDS algorithm thus has four adjustable parameters: n_{seg}, σ_{Sb}, f and N_{min}.

The step-by-step procedure to distribute lesions in the DNA segment is as follows:

(1) Select a nucleotide pair at random from the DNA segment, i.e., select a uniformly distributed integer in the range $[1, n_{seg}]$.
(2) Select one of two DNA strands at random. If the selected nucleotide is not already damaged, record the strand break at the location. Otherwise, go to step 1.
(3) Set $\sigma_{Sb} = \sigma_{Sb} - 1$. If $\sigma_{Sb} > 0$, go to step 1.
(4) Repeat steps 1 through 3 for σ_{Bd} base damages ($\sigma_{Bb} = f\sigma_{Sb}$).

In the original version of the MCDS algorithm (Semenenko and Stewart 2004), an additional step was included to scale the segment length and the number of strand breaks and base damages in proportion to absorbed dose (i.e., $N_{seg} = gn_{seg}D$, $\Sigma_{Sb} = g\sigma_{Sb}D$ and $\Sigma_{Bd} = g\sigma_{Bd}D$). An optional parameter, denoted by g, was also included in the original formulation of the algorithm to account for cell-specific information about DNA damage yields or DNA content (Semenenko and Stewart 2004). In this work, we dispense with these refinements and report damage yields per Gy per gigabase pair (Gbp).

The step-by-step procedure to group lesions into clusters (the second simulation stage) is as follows:

(1) Start at one end of the DNA segment and locate the first lesion on either or both strands. Set the start of the cluster to the location of the lesion(s).
(2) Starting with the base pair following the last identified lesion (upstream lesion), move along the DNA segment in the same direction and count the number of undamaged base pairs present before the next (downstream) lesion is encountered. If the end of the DNA segment is reached before encountering another lesion, set the end of the cluster to the location of the last detected lesion and quit.
(3) If the number of undamaged base pairs is $\geqslant N_{min}$, set the end position of the cluster to the location of the upstream lesion. Then, set the start position of the next cluster to the location of the downstream lesion.
(4) Go to step 2.

After all of the lesions in the DNA segment have been grouped into clusters, the cluster properties are analysed in terms of the nature and spatial distribution of the constituent lesions. A cluster is classified as a DSB if at least one strand break is found on each DNA strand within 10 bp. All clusters that contain at least one strand break but are not classified as DSBs are marked as SSBs. The remaining clusters are classified as 'base damage'.

2.2. Interpolation of damage yields from track-structure simulations

Figure 1 shows the Monte Carlo simulation data of Nikjoo *et al* (1994, 1997, 1999, 2001, 2002) and Friedland *et al* (2003, 2005) for SSB[2] and DSB yields plotted as a function of Z_{eff}^2/β^2. Here, Z_{eff} is the effective charge of the ion, which is less than the nuclear charge Z due to the effect of screening of nuclear charge by atomic electrons, and $\beta \equiv v/c$ is the velocity

[2] Unpublished results of simulations of SSB yields produced by α particles have been provided by Dr Werner Friedland.

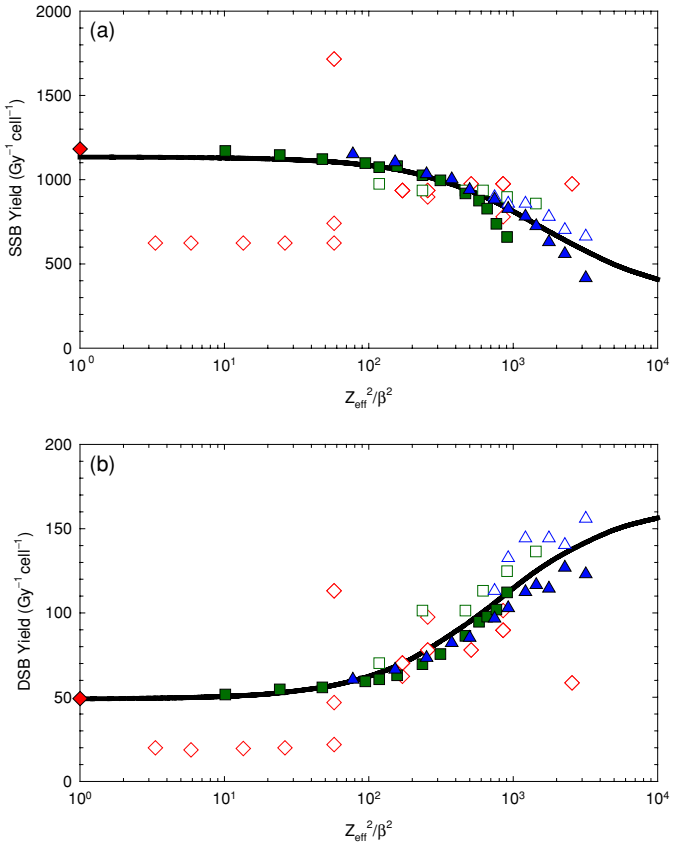

Figure 1. Dependence of SSB (a) and DSB (b) yields predicted by detailed Monte Carlo calculations of Nikjoo *et al* (1994, 1997, 1999, 2001, 2002) (open symbols) and Friedland *et al* (2003, 2005) (filled symbols) on Z_{eff}^2/β^2. The data from Nikjoo *et al* and Friedland *et al* were transformed into damage yields per average human cell by using conversion factors 3.9×10^{12} Da cell^{-1} and 6 Gbp cell^{-1}, respectively. Diamonds—electrons, squares—protons, triangles—α particles. Thick curves are fits to a function described by (3).

(This figure is in colour only in the electronic version)

v of the ion relative to the velocity of light in vacuum, c. The ratio Z_{eff}^2/β^2 is believed to provide an appropriate alternative to particle linear energy transfer (LET) for the comparison and interpolation of data (Katz 1970). The effective charge was calculated according to Barkas (1963)

$$Z_{\text{eff}} = Z[1 - \exp(-125 \cdot \beta \cdot Z^{-2/3})]. \tag{1}$$

The values of β were calculated with the equation

$$\beta = \sqrt{1 - \frac{1}{(1 + T/m_0c^2)^2}}, \tag{2}$$

where T is kinetic energy and $m_0$is the rest mass of the particle. The data for electrons were combined with those for protons and α particles by plotting strand break yields as a function of Z^2/β^2, where $Z = -1$ and β is defined by (2) with $m_0c^2 = 511$ keV.

With the exception of data of Nikjoo *et al* for electrons with energies ⩾4.5 keV (Nikjoo *et al* 1994, 1997, 1999, 2001, 2002), both sets of track-structure simulations form a continua of points that are well approximated by

$$f(x) = u + \frac{(v-u)x}{x+w}, \tag{3}$$

where $x \equiv Z_{\text{eff}}^2/\beta^2$. The thick line also shown in figure 1 is the damage yield predicted by equation (3) with $u = 1134$, $v = 291$, $w = 1615$ for SSBs and $u = 48.9$, $v = 164.5$, $w = 759$ for DSBs. Equation (3) has the useful property that $f(1) \approx f(0) = u$ and $f(\infty) = v$. The fits to the track-structure simulations suggest that, for all possible values of $x = Z_{\text{eff}}^2/\beta^2$, the number of SSBs is within the range between 291 Gy^{-1} cell^{-1} (48.5 Gy^{-1} Gbp^{-1}) and 1134 Gy^{-1} cell^{-1} (189 Gy^{-1} Gbp^{-1}). The DSB yields range between 48.9 Gy^{-1} cell^{-1} (8.15 Gy^{-1} Gbp^{-1}) and 164.5 Gy^{-1} cell^{-1} (27.4 Gy^{-1} Gbp^{-1}).

2.3. Estimation of parameters for the MCDS algorithm

Revised estimates of the MCDS parameters are based on the interpolated damage yields derived from track-structure simulations (thick line in figure 1). To estimate parameters from the MCDS algorithm, we minimized the following criterion:

$$C = \sum_{i=1}^{2} \frac{(O_i - E_i)^2}{E_i}. \tag{4}$$

Here, O_i is the yield of the ith type of damage obtained with the MCDS algorithm and E_i is the interpolated yield for the ith type of damage. In equation (4), indices 1 and 2 refer to the two types of clusters considered in this work, SSBs and DSBs. Optimization of criterion C (4) was repeated with the interpolated SSB and DSB yields corresponding to a number of Z_{eff}^2/β^2 values ranging between 1 and 10 000 and the best-fit values of MCDS parameters (n_{seg}, σ_{Sb} and N_{min}) were obtained as a function of Z_{eff}^2/β^2. Because endpoints describing DNA base damage were not available for the above optimization procedure, the previous estimate of $f = 3$ (Semenenko and Stewart 2004) was used in all calculations. We determined that for different sets of SSB and DSB yields corresponding to a single Z_{eff}^2/β^2 value, σ_{Sb} and N_{min} did not change significantly as a function of Z_{eff}^2/β^2 (data not shown). We then fixed σ_{Sb} and N_{min} at their approximate optimal values of 1300 Gy^{-1} cell^{-1} and $N_{\text{min}} =$ 9 bp, respectively, and performed minimization of (4) by adjusting n_{seg}. The values of n_{seg} can also be very reasonably approximated by (3) with $u = 149\,200$, $v = 25\,600$ and $w = 267$ (data not shown). We thus propose the following new inputs for the MCDS algorithm:

$$\begin{aligned} &\sigma_{\text{Sb}} = 1300\,\text{Gy}^{-1}\,\text{cell}^{-1}, \\ &f = 3, \\ &n_{\text{seg}}(x) = 149\,200 - \frac{123\,600x}{x+267}\,\text{bp}\,\text{Gy}^{-1}\,\text{cell}^{-1}, \qquad x \equiv \frac{Z_{\text{eff}}^2}{\beta^2}, \\ &N_{\text{min}} = 9\,\text{bp}. \end{aligned} \tag{5}$$

Because values of Z_{eff}^2/β^2 (or Z^2/β^2 for electrons) for the data used to obtain these parameter estimates (Nikjoo *et al* 1994, 1997, 1999, 2001, 2002, Friedland *et al* 2003, 2005) varied between ~1 and 3200, the new parameter estimates are most appropriate for $1 \leqslant Z_{\text{eff}}^2/\beta^2 \leqslant$ 3200. In terms of particle energy, the revised parameter estimates are valid for electrons and light ions with energies ranging from some minimum kinetic energy, T_{min}, which corresponds to the maximum Z_{eff}^2/β^2 value of 3200, to relativistic energies (~1 GeV) corresponding to small Z_{eff}^2/β^2 values. T_{min} is ~0.000 08 MeV, 0.105 MeV and 2 MeV for electrons, protons and α particles, respectively.

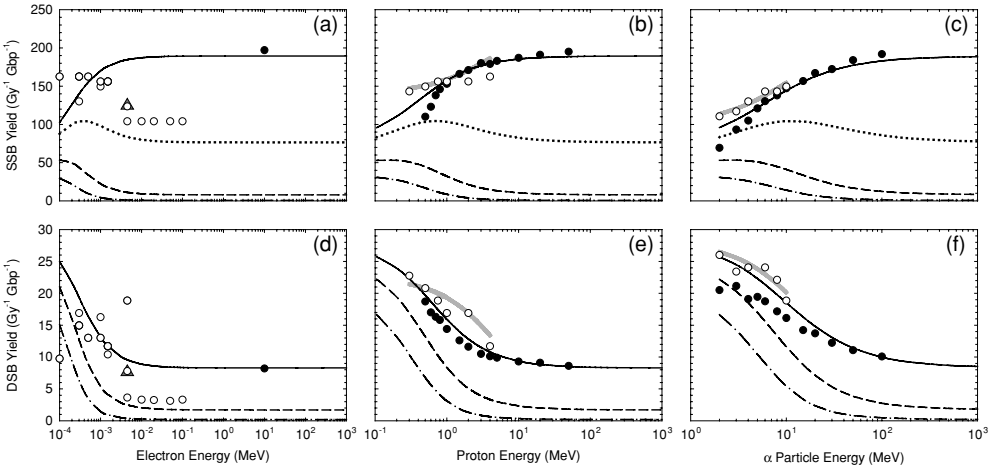

Figure 2. Comparison of SSB ((a), (b), (c)) and DSB ((d), (e), (f)) yields for electrons ((a), (d)), protons ((b), (e)) and α particles ((c), (f)) obtained with different models to calculate DNA damage. Open symbols—Nikjoo *et al* (1994, 1997, 1999, 2001, 2002), filled symbols—Friedland *et al* (2003, 2005), triangle (4.5 keV electrons) or thick line (protons and α particles)—Semenenko and Stewart (2004), solid line—this work. Dotted line—yield of SSBs/DSBs composed of more than one lesion, dashed line—more than three lesions, dash-dot line—more than five lesions.

2.4. Simulation of the effects of free radical scavengers

To simulate the effects of free radical scavengers, such as dimethyl sulfoxide (DMSO), we assumed that the numbers of strand breaks, σ_{Sb}, and base damages, σ_{Bd}, decrease as the scavenger concentration, $[S]$, increases. In particular, σ_{Sb} is multiplied by a dimensionless function:

$$h([S]) = \frac{\phi[S] + K}{[S] + K}. \tag{6}$$

The number of base damages distributed within the DNA segment (see step 4 in the corresponding algorithm described in section 2.1) is determined using $\sigma_{\mathrm{Bb}} = h([S]) \cdot f\sigma_{\mathrm{Sb}}$, where $f = 3$. In the limit when the scavenger concentration is zero, $h = 1$ and MCDS simulations correspond to a normal cellular environment. For very large scavenger concentrations, $h \to \phi$ and the numbers of strand breaks and base damages distributed within the DNA segment are $\phi\sigma_{\mathrm{Sb}}$ and $\phi f \sigma_{\mathrm{Sb}}$, respectively. Parameter ϕ thus represents the fraction of strand breaks and base damages that are not scavengeable. Parameter K may be interpreted as the concentration (in the same units as $[S]$) at which function h is reduced to its half-value, i.e., $(1 + \phi)/2$.

3. Results and discussion

Figure 2 shows SSB and DSB yields predicted by the MCDS algorithm with the new (5) and original (Semenenko and Stewart 2004) parameters in comparison with track-structure simulations of Nikjoo *et al* (1994, 1997, 1999, 2001, 2002) and Friedland *et al* (2003, 2005). The SSB and DSB yields predicted by the MCDS algorithm with the new set of parameters (5) are within the variation observed among the results for the track-structure simulations of Nikjoo *et al* (1994, 1997, 1999, 2001, 2002) and Friedland *et al* (2003, 2005), as expected since the new parameters are derived from the interpolated SSB and DSB damage yields (figure 1,

solid lines). In contrast, the original MCDS parameters (Semenenko and Stewart 2004) were derived from the results of simulations by Nikjoo *et al* (1999, 2001) and thus provide better agreement with that dataset than the new parameterization.

The comparison of results shown in figure 2 demonstrates that the MCDS algorithm can reproduce the overall trends in SSB and DSB yields predicted by track-structure simulations for electrons, protons and α particles over a wide range of energies using a common set of parameters, i.e., (5). Moreover, three out of the four MCDS parameters are the same for all three types of radiation (i.e., $\sigma_{\mathrm{Sb}} = 1300$ Gy^{-1} cell^{-1}, $f = 3$ and $N_{\mathrm{min}} = 9$ bp). The only parameter that depends on particle LET $\left(Z_{\mathrm{eff}}^2/\beta^2\right)$ is n_{seg}. This observation implies that the main difference between energetic electrons, protons and α particles is the degree of lesion clustering. The lesion clustering aspects of the damage formation process can be adequately modelled by introducing a single parameter, n_{seg}, that depends on the ratio $Z_{\mathrm{eff}}^2/\beta^2$.

The commonality of the σ_{Sb}, f and N_{min} parameters for all three types of radiation has the important consequence that the overall SSB and DSB yields approach common asymptotes in the limit when the kinetic energy becomes very large (small values for $Z_{\mathrm{eff}}^2/\beta^2$). For relativistic electrons, protons and α particles, the SSB yield approaches ~189 SSBs Gy^{-1} Gbp^{-1} and the DSB yield approaches ~8.3 DSBs Gy^{-1} Gbp^{-1} (SSB to DSB ratio is ~23). Studies of the relative biological effectiveness (RBE) for cell inactivation provide indirect support for the idea that energetic light ions produce damage similar to low-LET radiation. For example, Robertson *et al* (1994) report that RBE, with ^{60}Co γ rays as a reference radiation, decreases to 1.2 for the high-energy portion of the mixed field of 200 MeV protons compared to more than 1.3 for the low-energy portion of the field. In a study by Furusawa *et al* (2000), cell survival parameters (α and D_0) for V79 Chinese hamster and human salivary gland tumour cells exposed to ^{3}He ions approach those determined for 200 kVp x-rays as the energy of the ^{3}He ions increases. Microdosimetric lineal energy spectra also provide evidence that high-energy protons can be considered a low-LET radiation (Robertson *et al* 1994).

As a further test of the new MCDS parameterization, we compared the per cent yields of simple and complex SSBs and DSBs predicted by the MCDS algorithm to the damage yields reported by Nikjoo *et al* (2001). This test of the algorithm is especially useful because the damage yields reported in Nikjoo *et al* (2001) were not used to estimate parameters for the MCDS algorithm reported in this paper. The comparison of results in figure 3 demonstrates that the relative damage yields predicted using the new MCDS parameters give reasonable agreement with the detailed Monte Carlo simulations. The new parameterization improves the agreement between MCDS results and the data of Nikjoo *et al* (2001) for some endpoints and radiation types (e.g., relative yields of DSB, SSB$_{\mathrm{c}}$ and DSB$_{\mathrm{c}}$ are improved for protons and α particles, but not electrons) while for other damage configurations (e.g., SSB$_{\mathrm{cb}}$) the trend is reversed. Overall, the new parameterization provides as good agreement with the detailed track-structure simulation results as the parameters reported in Semenenko and Stewart (2004).

The rate of DSB rejoining tends to decrease with increasing damage complexity (Pastwa *et al* 2003), and the probability of correct SSB or base damage repair tends to decrease as the number of lesions per cluster increases (Semenenko *et al* 2005, Semenenko and Stewart 2005). The complexity of radiation-induced DNA damage therefore has a large impact on repair fidelity. In addition to total SSB and DSB yields, figure 2 shows the predicted yield of complex SSBs and DSBs or sites of base damage. Electrons with kinetic energies greater than about 100 keV form less than 1 DSB Gy^{-1} Gbp^{-1} with more than five base damages or strand breaks per cluster. Similarly, protons with kinetic energies greater than about 10 MeV and α particles with kinetic energies greater than 100 MeV form less than one very complex DSB Gy^{-1} Gbp^{-1}. The formation of complex SSBs increases as particle energy decreases (figures 2(a)–(c)). The average number of lesions per cluster (figure 4) and the average cluster length (figure 5)

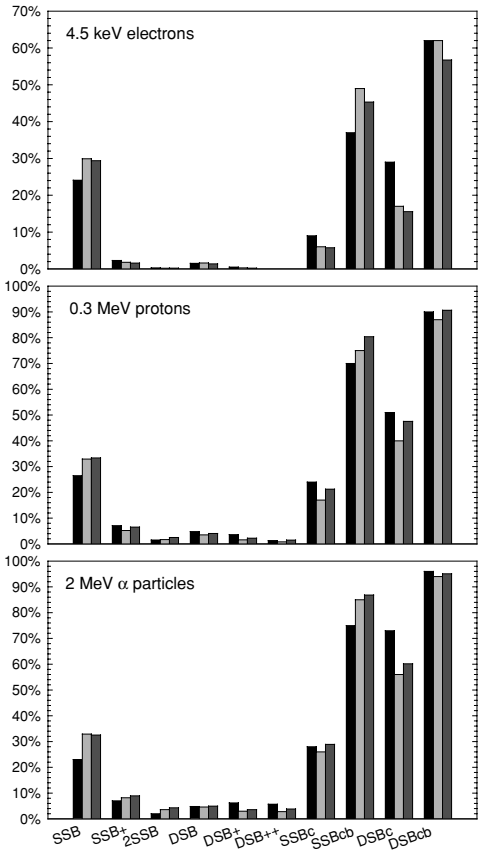

Figure 3. Comparison of DNA damage spectra predicted by Nikjoo *et al* (2001) (black bars), Semenenko and Stewart (2004) (light grey bars) and this work (dark grey bars) for 4.5 keV electrons, 0.3 MeV protons and 2 MeV α particles. For a description of damage categories, see Nikjoo *et al* (2001).

also tend to increase with decreasing particle energy. These observations all suggest that the most complex, difficult-to-repair forms of DNA damage are produced at the end of a charged particle's track.

DSB measurements performed by Newman *et al* (2000) indicate that 3.5 MeV α particles produce approximately 12 DSBs per Gy per Gbp of DNA in V79 Chinese hamster cells. Studies reported by Rydberg *et al* (2002) give estimates of 10.4–11.8 DSBs Gy^{-1} Gbp^{-1} for GM38 human skin fibroblasts irradiated with 3–7 MeV α particles. For comparison, the MCDS algorithm predicts 20–24 DSBs Gy^{-1} Gbp^{-1} for the same range of α-particle energies, a factor of 2 higher. Belli *et al* (2002) detected 13.1 DSBs Gy^{-1} Gbp^{-1} after irradiation of V79 cells with $\sim$0.7 MeV protons. In contrast, the MCDS-predicted value for 0.7 MeV protons is 36% higher, i.e., 17.8 DSBs Gy^{-1} Gbp^{-1}. The asymptotic value of 8.3 DSBs Gy^{-1} Gbp^{-1} for high-energy electrons can be compared to measured data for energetic photons, such as those produced by ^{60}Co sources. Experimental DSB yields for ^{60}Co γ rays vary between 5.8 and 6.8 Gy^{-1} Gbp^{-1} (Höglund *et al* 2000, Belli *et al* 2002, Dini *et al* 2005, Kühne *et al* 2005). These values are intermediate between the simulation results of Nikjoo *et al* for electrons with energies up to 100 keV (Nikjoo *et al* 2002) and values for high-energy electrons ($\geqslant$10 MeV)

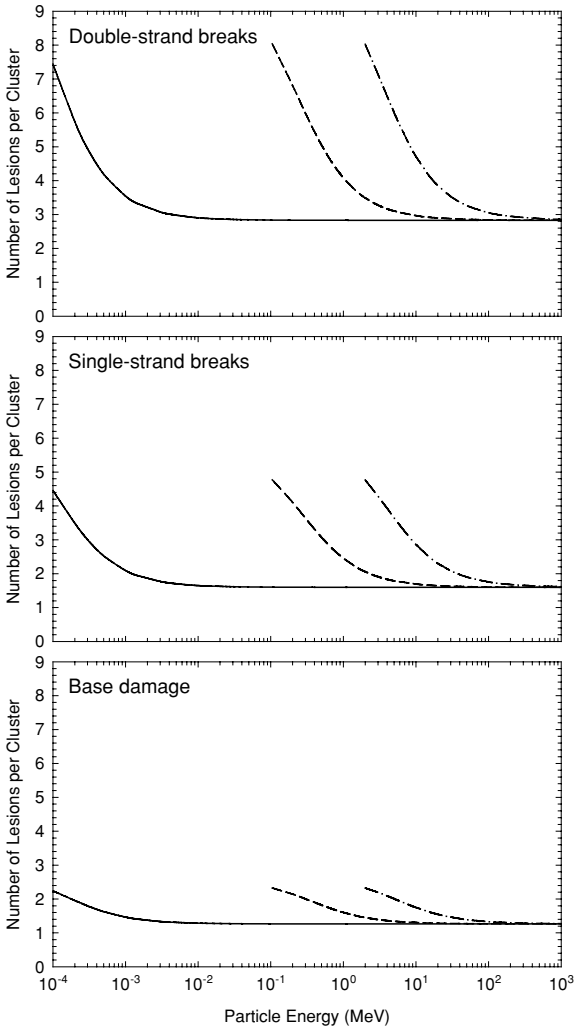

Figure 4. The average number of lesions per DSB, SSB and site of multiple base damage. Solid line—electrons, dashed line—protons, dash-dot line—α particles.

obtained in this study and in Friedland *et al* (2003). Because track-structure simulations often give only approximate numerical agreement with measured DSB yields (e.g., see Rydberg *et al* (2002), Friedland *et al* (2003, 2005)), the differences in measured and MCDS-predicted DSB yields are not surprising. That is, parameters used in the MCDS algorithm were selected to reproduce results from track-structure simulations rather than measured data. The observed difference in measured and predicted DSB yields may be attributed to the loss of small fragments in the pulsed-field gel electrophoresis (PFGE) assay (Rydberg *et al* 2002, Friedland *et al* 2005), although some of these differences may also be due to simplifications inherent in any model, including track-structure simulations. Also, it is worth noting that RBE values predicted by Monte Carlo track-structure calculations compare favourably to measured data for protons (Friedland *et al* 2003). Regardless, the inconsistencies in measured and predicted absolute DSB yields merit closer examination in the future.

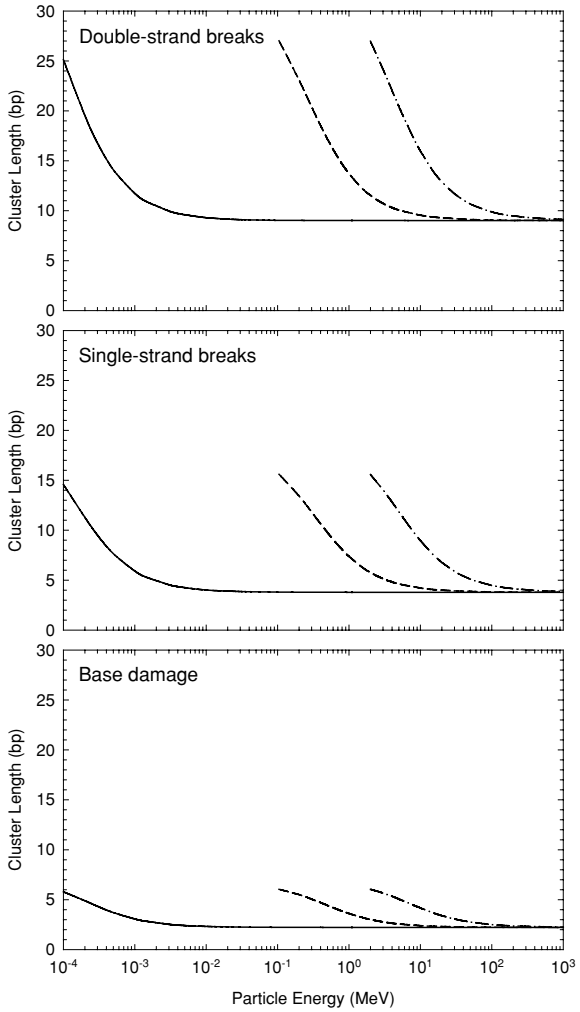

Figure 5. The average cluster length for DSBs, SSBs and sites of multiple base damage. Solid line—electrons, dashed line—protons, dash-dot line—α particles.

The track-structure calculations used to estimate MCDS parameters (Nikjoo *et al* 1994, 1997, 1999, 2001, 2002, Friedland *et al* 2003, 2005) account for the direct and indirect (free radical-mediated) mechanisms of DNA damage production. Because the MCDS algorithm reproduces the results of track-structure calculations, the MCDS simulations implicitly account for both direct and indirect DNA damage mechanisms. To examine the effects on damage complexity of the direct and indirect mechanisms, the MCDS algorithm was modified to mimic reductions in the amount of strand breaks and base damages associated with exposure to an extrinsic free radical scavenger (see section 2.4 in methods), DMSO. DMSO is an efficient OH-radical scavenger (Reuvers *et al* 1973) that offers protection against both strand breakage and base damage (Skov 1984).

Figure 6 compares the MCDS-predicted relative DSB yield as a function of DMSO concentration to the measured data of deLara *et al* (1995) for V79 Chinese hamster fibroblasts. MCDS simulations were performed for 3.31 MeV α particles (the mean energy of a ^{238}Pu

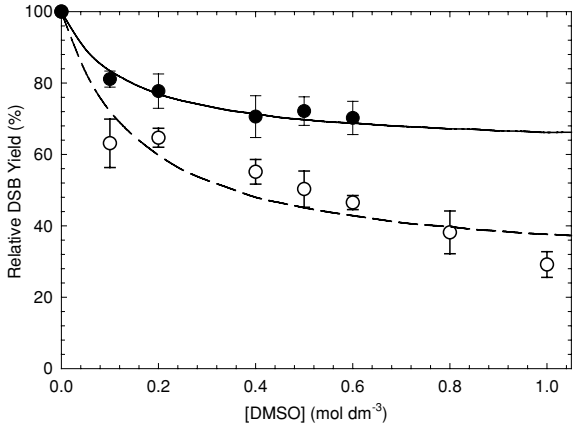

Figure 6. Comparison of MCDS-predicted relative DSB yields as a function of DMSO concentration with published experimental data. Symbols show data of deLara *et al* (1995) obtained by irradiating V79 hamster cells with ^{238}Pu α particles (filled symbols) and ^{137}Cs γ rays (open symbols). Solid line was obtained by simulating DNA damage for 3.31 MeV α particles with $\phi = 0.75$ and $K = 0.14$ mol dm^{-3}. Dashed line—0.5 MeV electrons, $\phi = 0.52$ and $K = 0.21$ mol dm^{-3}.

source used by deLara *et al*) and 0.5 MeV electrons (used to approximate the quality of radiation emitted by a ^{137}Cs source). The relative yield was determined as a ratio of the DSB yield for the specified DMSO concentration to the DSB yield at zero concentration (i.e., a normal cellular environment). Figure 6 shows that MCDS simulations can reasonably approximate the experimental data obtained with ^{137}Cs γ rays ($\phi = 0.52$, $K = 0.21$ mol dm^{-3}) and ^{238}Pu α particles ($\phi = 0.75$, $K = 0.14$ mol dm^{-3}). Since OH radicals are the main species mediating the indirect effects of ionizing radiation (Roots and Okada 1975), the parameter ϕ may be interpreted, when DMSO is the scavenger, as the upper bound of the fraction of DNA damage produced through the direct mechanism. Our analyses suggest that radiation of high LET may produce more damage through the direct mechanism (up to 75%) compared to low-LET radiation (up to 52%). These estimates are consistent with observations of Roots *et al* (1985), who reported that the fraction of the indirect effect (measured as OH-mediated cell killing) decreases from ~55% for x-rays to ~23% for radiation with LET $\geqslant$100 keV μm^{-1}, i.e., the direct effect fraction increases from ~45% to ~77%. However, larger estimates of the fraction of cell killing mediated by indirect action of radiation, i.e., up to 65%, have also been reported in the literature (Ward 1998).

Figure 7 shows the predicted spectra of DNA damage formed by 0.5 MeV electrons and 3.31 MeV α particles under a normal cellular environment and under conditions when the direct effect is predominant, i.e., when [DMSO] $= \infty$. The values of ϕ and K used for these simulations are the same as those used in figure 6 (i.e., $\phi = 0.75$ and $K = 0.14$ mol dm^{-3} for 3.31 MeV α particles and $\phi = 0.52$ and $K = 0.21$ mol dm^{-3} for 0.5 MeV electrons). The model predicts that DMSO decreases the overall complexity of the DNA damage formed by low- and high-LET radiation. Addition of the OH-radical scavenger has a larger impact on the yields of DNA damage when cells are exposed to low-LET radiation (0.5 MeV electrons) compared to high-LET radiation (3.31 MeV α particles). The relative yields of more complex types of damage (SSB+, 2SSB, DSB+, DSB++) are affected by addition of DMSO to a larger extent than simple DNA breaks (SSB, DSB).

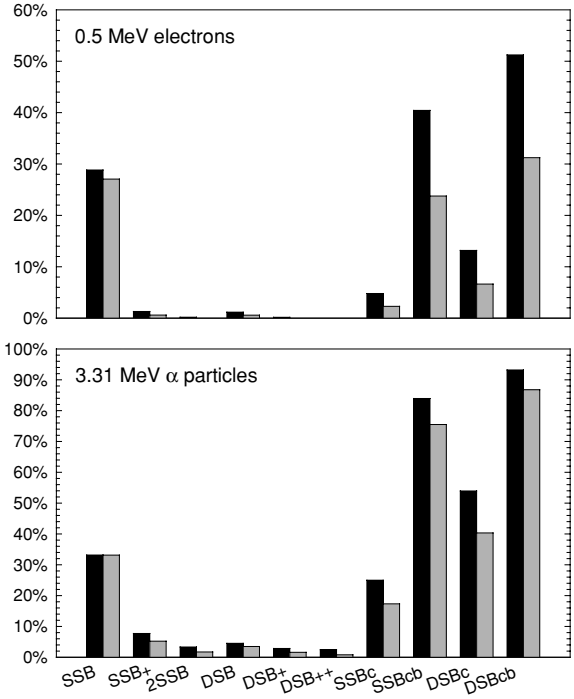

Figure 7. Comparison of DNA damage spectra predicted by the MCDS algorithm for normal cellular environment, i.e., [DMSO] = 0 (dark bars) and for high scavenging conditions, i.e., [DMSO] = ∞ (light bars).

4. Conclusions

Because of limitations in the commonly used DNA damage assays, such as PFGE, information about lesion clustering within one or two turns of the DNA cannot be easily determined through direct experimentation. However, Monte Carlo track-structure simulations of the physical and chemical processes initiated by ionizing radiation can provide such information with a minimal number of adjustable parameters. In this paper, we have demonstrated that the overall yields of SSBs and DSBs, as well as the local complexity of clusters, predicted by track-structure simulations can be interpolated and extended using a very fast, quasi-phenomenological Monte Carlo scheme, i.e., the MCDS algorithm[3]. Moreover, three of the four parameters used in the MCDS algorithm are the same ($\sigma_{\mathrm{Sb}} = 1300$ Gy^{-1} cell^{-1}, $f = 3$ and $N_{\mathrm{min}} = 9$ bp) for electrons, protons and α particles. The fourth parameter (n_{seg}), which depends on the ratio $Z^2_{\mathrm{eff}}/\beta^2$, characterizes the degree of damage clustering within one or two turns of the DNA. This observation suggests that the absolute yield of strand breaks and base damage is approximately the same, per Gy per Gbp, for electrons and energetic light ions but the degree of lesion clustering on a nanometre scale (10–20 bp) is quite different for low- and high-LET radiation. For proton therapy and other treatment modalities involving high-energy ions, the reported studies suggest that the damage formed within the tumour (end of the ion track) is substantially more complex than the damage formed within normal tissues (start of the ion track). Analysis of published DSB induction data obtained at different DMSO concentrations

[3] A computer program implementing the MCDS algorithm is available at http://rh.healthsciences.purdue.edu/mcds/.

suggests that the indirect effect of ionizing radiation contributes to the formation of more complex forms of DNA strand breaks.

Acknowledgments

The authors wish to thank Dr Werner Friedland at GSF—National Research Center for Environment and Health, Neuherberg, Germany for providing simulated damage induction data for α particles and Dr Michael Dingfelder at East Carolina University for helpful discussions. This work is supported by the Office of Science (BER), US Department of Energy, grant nos. DE-FG02-03ER63541 and DE-FG02-03ER63665.

References

Amaldi U and Kraft G 2005 Radiotherapy with beams of carbon ions *Rep. Prog. Phys.* **68** 1861–82

Barkas W H 1963 *Nuclear Research Emulsions* vol 1 (New York: Academic) p 371

Belli M, Cherubini R, Dalla Vecchia M, Dini V, Esposito G, Moschini G, Sapora O, Simone G and Tabocchini M A 2002 DNA fragmentation in V79 cells irradiated with light ions as measured by pulsed-field gel electrophoresis: I. Experimental results *Int. J. Radiat. Biol.* **78** 475–82

deLara C M, Jenner T J, Townsend K M, Marsden S J and O'Neill P 1995 The effect of dimethyl sulfoxide on the induction of DNA double-strand breaks in V79-4 mammalian cells by alpha particles *Radiat. Res.* **144** 43–9

Dini V, Antonelli F, Belli M, Campa A, Esposito G, Simone G, Sorrentino E and Tabocchini M A 2005 Influence of PMMA shielding on DNA fragmentation induced in human fibroblasts by iron and titanium ions *Radiat. Res.* **164** 577–81

Friedland W, Dingfelder M, Jacob P and Paretzke H G 2005 Calculated DNA double-strand break and fragmentation yields after irradiation with He ions *Radiat. Phys. Chem.* **72** 279–86

Friedland W, Jacob P, Bernhardt P, Paretzke H G and Dingfelder M 2003 Simulation of DNA damage after proton irradiation *Radiat. Res.* **159** 401–10

Furusawa Y, Fukutsu K, Aoki M, Itsukaichi H, Eguchi-Kasai K, Ohara H, Yatagai F, Kanai T and Ando K 2000 Inactivation of aerobic and hypoxic cells from three different cell lines by accelerated ^{3}He-, ^{12}C- and ^{20}Ne-ion beams *Radiat. Res.* **154** 485–96

Höglund E, Blomquist E, Carlsson J and Stenerlöw B 2000 DNA damage induced by radiation of different linear energy transfer: initial fragmentation *Int. J. Radiat. Biol.* **76** 539–47

Holley W R and Chatterjee A 1996 Clusters of DNA damage induced by ionizing radiation: formation of short DNA fragments. I. Theoretical modeling *Radiat. Res.* **145** 188–99

Katz R 1970 RBE, LET and $z/\beta^{\alpha *}$ *Health Phys.* **18** 175

Kühne M, Urban G, Frankenberg D and Löbrich M 2005 DNA double-strand break misrejoining after exposure of primary human fibroblasts to C_K characteristic X rays, 29 kVp X rays and ^{60}Co γ rays *Radiat. Res.* **164** 669–76

Newman H C, Prise K M and Michael B D 2000 The role of higher-order chromatin structure in the yield and distribution of DNA double-strand breaks in cells irradiated with X-rays or α-particles *Int. J. Radiat. Biol.* **76** 1085–93

Nikjoo H, Bolton C E, Watanabe R, Terrissol M, O'Neill P and Goodhead D T 2002 Modelling of DNA damage induced by energetic electrons (100 eV to 100 keV) *Radiat. Prot. Dosim.* **99** 77–80

Nikjoo H, O'Neill P, Goodhead D T and Terrissol M 1997 Computational modelling of low-energy electron-induced DNA damage by early physical and chemical events *Int. J. Radiat. Biol.* **71** 467–83

Nikjoo H, O'Neill P, Terrissol M and Goodhead D T 1994 Modelling of radiation-induced DNA damage: the early physical and chemical event *Int. J. Radiat. Biol.* **66** 453–7

Nikjoo H, O'Neill P, Terrissol M and Goodhead D T 1999 Quantitative modelling of DNA damage using Monte Carlo track structure method *Radiat. Environ. Biophys.* **38** 31–8

Nikjoo H, O'Neill P, Wilson W E and Goodhead D T 2001 Computational approach for determining the spectrum of DNA damage induced by ionizing radiation *Radiat. Res.* **156** 577–83

Pastwa E, Neumann R D, Mezhevaya K and Winters T A 2003 Repair of radiation-induced DNA double-strand breaks is dependent upon radiation quality and the structural complexity of double-strand breaks *Radiat. Res.* **159** 251–61

Reuvers A P, Greenstock C L, Borsa J and Chapman J D 1973 Studies on the mechanism of chemical radioprotection by dimethyl sulphoxide *Int. J. Radiat. Biol. Relat. Stud. Phys. Chem. Med.* **24** 533–6

Robertson J B, Eaddy J M, Archambeau J O, Coutrakon G B, Miller D W, Moyers M F, Siebers J V, Slater J M and Dicello J F 1994 Relative biological effectiveness and microdosimetry of a mixed energy field of protons up to 200 MeV *Adv. Space Res.* **14** 271–5

Roots R, Chatterjee A, Chang P, Lommel L and Blakely E A 1985 Characterization of hydroxyl radical-induced damage after sparsely and densely ionizing irradiation *Int. J. Radiat. Biol. Relat. Stud. Phys. Chem. Med.* **47** 157–66

Roots R and Okada S 1975 Estimation of life times and diffusion distances of radicals involved in X-ray-induced DNA strand breaks of killing of mammalian cells *Radiat. Res.* **64** 306–20

Rydberg B, Heilbronn L, Holley W R, Löbrich M, Zeitlin C, Chatterjee A and Cooper P K 2002 Spatial distribution and yield of DNA double-strand breaks induced by 3–7 MeV helium ions in human fibroblasts *Radiat. Res.* **158** 32–42

Semenenko V A and Stewart R D 2004 A fast Monte Carlo algorithm to simulate the spectrum of DNA damages formed by ionizing radiation *Radiat. Res.* **161** 451–7

Semenenko V A and Stewart R D 2005 Monte Carlo simulation of base and nucleotide excision repair of clustered DNA damage sites: II. Comparisons of model predictions to measured data *Radiat. Res.* **164** 194–201

Semenenko V A, Stewart R D and Ackerman E J 2005 Monte Carlo simulation of base and nucleotide excision repair of clustered DNA damage sites: I. Model properties and predicted trends *Radiat. Res.* **164** 180–93

Skov K A 1984 The contribution of hydroxyl radical to radiosensitization: a study of DNA damage *Radiat. Res.* **99** 502–10

Tomita H, Kai M, Kusama T, Aoki Y and Ito A 1994 Monte Carlo simulation of DNA strand breaks induced by monoenergetic electrons using higher-order structure models of DNA *Int. J. Radiat. Biol.* **66** 669–82

Ward J F 1998 Nature of lesions formed by ionizing radiation *DNA Damage and Repair: DNA Repair in Higher Eukaryotes* vol 2 ed J A Nickoloff and M F Hoekstra (Totowa, NJ: Humana Press) pp 65–84